J Appl Electrochem (2010) 40:2051–2059
DOI 10.1007/s10800-010-0186-7

ORIGINAL PAPER

Electrolytic preparation of cyclic multilayer Zn–Ni alloy coating using switching cathode current densities

K. Venkatakrishna · A. Chitharanjan Hegde

Received: 2 April 2010 / Accepted: 5 September 2010 / Published online: 18 September 2010

Abstract Cyclic multilayer alloy (CMA) coating of Zn–Ni was developed on mild steel using single bath technique, by proper manipulation of cathode current densities. The thickness and composition of the individual layers were altered precisely and conveniently by cyclic modulation of cathode current densities. Multilayer coatings, having sharp change in compositions were developed using square current pulses. Gelatin and sulphanilic acid (SA) acid were used as additives. Laminar deposits with different configurations were produced, and their corrosion behaviors were studied, in 5% NaCl solution by electrochemical methods. It was observed that the corrosion resistance of CMA coating increased progressively with number of layers (up to certain optimal numbers) and then decreased. Cyclic voltammetry study demonstrated the role of gelatin and SA in multilayer coating. The coating configuration has been optimized for the peak performance against corrosion. The substantial decrease of corrosion rate, in the case of multilayer coatings was attributed to the changed intrinsic electric properties, evidenced by Electrochemical Impedance Spectroscopy (EIS) study. The surface morphology and its roughness were examined by Atomic Force Microscopy (AFM). The surface and cross-sectional view of coatings were examined, using Scanning Electron Microscopy (SEM). X-ray photoelectron spectrum (XPS) study was carried out for surface analysis. The relative performance of pure Zn, monolithic and CMA coatings were compared and discussed.

K. Venkatakrishna · A. Chitharanjan Hegde (✉)
Electrochemistry Research Laboratory, Department of Chemistry, National Institute of Technology Karnataka, Srinivasnagar 575 025, India
e-mail: achegde@rediffmail.com

Keywords Multilayered Zn–Ni alloy · Switching current densities · Corrosion study

1 Introduction

Recently, electrodeposition of composition modulated multilayered alloys (CMMA) of Zn–M (where M = Fe group metals like Ni, Co and Fe) has received more attention in surface engineering because of their excellent corrosion resistance, increased mechanical strength and micro hardness etc. [1, 2]. Codeposition of two metals requires that their individual reversible potentials are reasonably close to each other in the specific bath. This is the case when their standard potentials are close, when the concentration of one of the metals in solution is properly tuned, or when complexing agent that forms complexes with different stability constants is added. Eliaz and Gileadi [3] have recently reviewed the principles of alloy codeposition and the phenomenon of anomalous codeposition (ACD) in the frame work of a more comprehensive review of induced codeposition. The term anomalous codeposition was coined by Brenner [4] to describe an electrochemical deposition process in which the less noble metal is deposited preferentially under most plating conditions. This behavior is typically observed in codeposition of iron group metals or in codeposition of iron group metal with Zn [5, 6].

There are two major ways to produce CMA electrodeposits. One of which is the dual bath technique (DBT), and other one is single bath technique (SBT) [7, 8]. The DBT involves the deposition of constituents from two separate plating baths in an alternate manner. Any combination of layers can be formed, provided that each can be individually deposited, and very thin metal or alloy films can easily be formed. However, DBT has some drawbacks. First it is

difficult to achieve the appropriate structure because of the periodic exposure of the substrate to potential contaminants during the transfer from one bath to another. In addition, the process might be more time consuming and difficult to automate in comparison to the alternate technique. In SBT, the metal ions required to form both deposit layers are contained in the single electrolyte and the alloy deposition is achieved by alternately changing the plating current/potential, possibly in combination with a modulation of the mass transport towards the cathode [9–11]. Although significant success has been achieved with the SBT, the selection of constituents is limited because their deposition potentials must be sufficiently different to allow a separate deposition of each. Difficulties can also be encountered in the deposition of very thin layers due to the less relaxation time for the redistribution of solutes in the diffusion double layer. In addition to that, it also difficult to get the layers of individual metals but most of they will be in the alloy form. However, it is possible to develop multilayered coatings of graded or altering composition from the single bath solution, by changing alternatively the cathode current densities [12].

A good number of investigators have examined the Cu–Ni multilayer system. Baral and Maxmovitch [13] were one of the first investigators to examine this particular system. They also developed a dual bath configuration for depositing successive layers of zinc and nickel with individual layer thicknesses of 20–500 nm, using a rotating disc electrode. Kalantary et al. [14] obtained Zn–Co CMA coatings with an overall thickness of 8 μm by electrodepositing alternate layers of zinc and nickel from the zinc sulphate and nickel sulphate electrolytes. Chawa et al. [7] reported the corrosion resistance of Zn–Co CMA coatings from zinc sulphate and nickel sulphamate baths showing better corrosion resistance, compared to that of monolithic Zn–Co coatings of similar thickness. Recently, Liao et al. [15–17] have studied both SBT and DBT of Zn/Zn–Fe and only Zn–Fe systems. Kirilova et al. [18–20] reported CMA coatings of Zn–Co from SBT. Recently, Thangaraj et al. [21] optimized a chloride bath for the production of Zn–Fe CMA coatings over mild steel, and showed that coating were found to have ~45 times better corrosion stability than monolithic Zn–Fe coatings of same thickness. Though improvement in corrosion resistance of Zn–Ni CMA electrodeposits, were widely reported, very little was done with regard to optimization of the deposition condition, using SBT to achieve the peak performance against corrosion.

2 Experimental

Polished mild steel panels with active surface area of 2.5 × 3 cm^2 were used for electrodeposition. Electrolytes were prepared using Laboratory Reagent (LR) grade chemicals (Merck, India) and distilled water. Gelatin and SA were used as primary and secondary additives, respectively. The electrodepositions (both monolithic and multilayer) were carried out in a rectangular PVC cell containing 250 cm^3 electrolyte solution, in conjunction with an adjustable power source (AGILENT N6705A). All depositions were carried out galvanostatically in a constantly stirred electrolyte, maintained at pH 3.5 and temperature 30 °C, for a duration of 10 min, for comparison purpose. The electrochemical characterization of the coatings were made using Galvanostat/Potentiostat (VersaSTAT^3, Princeton Applied Research).

Generally, in electroplating, the direct current (DC) or constant current results in the coatings having constant composition, called monolithic, or alternatively monolayer coatings, represented by notation, DC (Zn–Ni). Periodic change in the current density (c.d.) allows the growth of layers on substrate with periodic change in the chemical compositions. Due to the fact that the deposition of Zn–Ni alloys follow peculiar anomalous codeposition, the wt% Zn decreases, as the c.d. increases [4]. Or, in other words, Ni content increases. This decrease of more readily depositable (mrd) metal, in the deposit towards high c.d. is due to rapid depletion of ions (Zn^{+2} ions) [5]. Accordingly, the pulses of low c.d. resulted in layers with low Ni concentration, whereas pulses of high c.d. resulted in layers with higher Ni concentration. The instrument was set to cycle between two different cathode current densities, called switching cathode current densities (SCCD's) in a repetitive way. While the thickness of the each layer was controlled by the duration of one c.d., the composition of each layer is decided by the applied c.d. The total number of layers was fixed appropriately by adjusting the time for each cycle. Thus, CMA coatings of different configurations were produced. Such multilayer coatings are hereafter represented as, $(Zn–Ni)_{1/2/n,}$ where (Zn–Ni) represents alloy of Zn and Ni, and 1 and 2 represent the cathode c.d. that is made to cycle, and '*n*' represents the total number of layers formed during total deposition time (10 min). The composition of the bath, used for deposition of both monolayer and multilayer coatings is shown in the Table 1.

Cyclic voltammetry (CV) was performed in a conventional three-electrode cell, to better understand the process of electrodeposition, and to identify the effects of gelatin and SA. The bath composition and pH was maintained same, as in Table 1. Before carrying out the experiments, the bath temperature was stabilized at 30 °C. All chemicals used were of analytical grade. Double distilled water was used for preparation of the electrolyte solutions. Pure platinum foil with a surface area of 1 cm^2 was used as working electrode. Although this is a different material than the steel substrate used for galvanostatic deposition, it enabled elimination of noise in the CV experiments.

Table 1 Composition and operating parameters of optimized bath for electrodeposition of bright monolithic and CMA coatings of Zn–Ni alloy on mild steel

Bath composition	Amount (M)	Operating parameters
Zinc chloride	0.37	pH: 3.5
Nickel chloride	0.34	Temperature: 303 K
Ammonium chloride	2.24	Anode: Pure zinc
Potassium chloride	1.61	Current density, *i*: 30 mA cm^{-2}
Sulphanilic acid	0.03	
Gelatin	7 g l^{-1}	

Furthermore, it may be argued that once several nanometers of coating material are deposited, the substrate no longer has any effect on the deposition process. Before each experiment, the electrode was activated by immersion in dilute HNO_3. The CV experiments were conducted in a quiescent solution, without purging. A scan rate of 10 mV s^{-1} was selected based on preliminary experiments. The scan began from 0 V in the positive direction, up to +1.0 V. Then, it was reversed to the negative direction, down to –1.4 V, and finally reversed back to +1.0 V. The potentials were measured versus a saturated calomel reference electrode (SCE).

The corrosion studies were carried out at 25 °C in 5% NaCl solution at pH 6.0, prepared in distilled water. Cathodic and anodic polarization curves were obtained at scan rate of 1 mV s^{-1} by using SCE as reference, and platinum electrode as counter. The impedance behavior of the deposits was studied by drawing the Nyquist plot in the frequency range from 100 kHz to 10 MHz. The surface morphology of the coatings was also studied in air by Atomic Force Microscopy (AFM, PicoSPM^{TM} from Molecular Imaging). X-ray Photoelectron Spectroscopy (XPS) measurements were performed in UHV (2.5×10^{-10} Torr base pressure), using a 5600 Multi-Technique System (PHI, USA). The surface morphology of electroplates were studied by Scanning Electron Microscopy (SEM, JEOL 6380 LA).

3 Results and discussion

3.1 Bath chemistry

There is no available literature, with regard to the use of gelatin and SA in combination, as additives for electroplating of CMA Zn–Ni alloy. It was observed that gelatin has improved the homogeneity, and SA has enhanced the brightness of the coatings. Therefore, it was tried to understand whether SA acted as a brightener only, or also as a complexing agent. Gelatin is sometimes added to electroplating bath to control the deposition rate, crystallization, leveling and brightness of the deposit. Due to its very high molecular weight, its content in the plating baths in the present study represents concentrations, which were several orders of magnitude smaller than the concentrations of the zinc and nickel ions. Sulphanilic acid (SA, $NH_2C_6H_4SO_3H$, with IUPAC name, *p*-aminobenzene sulphonic acid) has a relatively high melting point (288 °C) and moderate solubility in water (>20 g L^{-1} at 25 °C). To demonstrate role of gelatin and SA, cyclic voltammetry study has been carried out with Zn–Ni bath, using smooth platinum (Pt) as working electrode at pH = 3.5, T = 30 °C, at scan rate, v = 10 mV s^{-1}.

Figure 1 shows the cyclic voltammograms obtained for Zn–Ni on Pt. without additives, the deposition started at approximately −1.15 V. The anodic sweep showed two dissolution peaks, the left must be associated with a Zn–Ni phase while the right may be associated either with another Zn–Ni phase or with pure Ni. The addition of SA shifted the deposition potential in the negative direction, starting at around −1.21 V, and made the peak more distinct. In the anodic sweep, a shoulder appeared at −0.8 V, while the area below the peak at −0.51 V decreased. The presence of gelatin changed the shape of the voltammograms in two ways: (i) the deposition potential was shifted to slightly less negative value (starting at around −1.13 V) while the deposition current density was decreased, and (ii) the intensity of the peaks in the anodic sweep was reduced while the left peak shifted to a more negative value (−0.89 V). The effect of gelatin was more pronounced than that of SA in the bath containing these two additives. Thus, it seems that SA along with gelatin affected the codeposition process by bringing large difference in reduction potential of Zn and Ni, and indirectly allowed

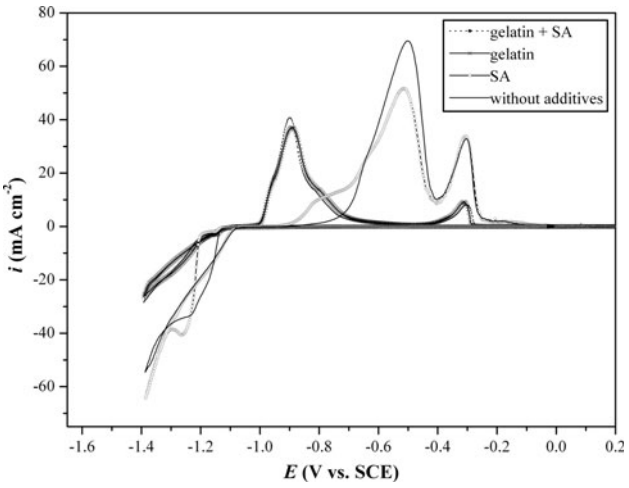

Fig. 1 Cyclic voltammograms for Zn–Ni bath, demonstrating the effects of gelatin and SA. Working electrode: Pt, pH = 3.5, T = 30 °C, u = 10 mV s^{-1}

greater provision for modulation in composition of the CMA coatings.

3.2 Monolithic Zn–Ni coating

A stable chloride bath was optimized using standard Hull cell method. The bath composition and operating parameters are as shown in the Table 1. Bright and uniform monolithic Zn–Ni alloy deposits were developed on mild steel at c.d. of 30 mA cm^{-2}, using SA as additive. At optimal condition, the deposit found to have 3.8 wt% Ni with corrosion rate 21.4 $\times$ 10^{-2} mm $year^{-1}$. The variation in the corrosion stability of the coatings, at different c.d. may be attributed to the difference in the phase structures of the deposits.

The XRD patterns of Zn–Ni alloy obtained at different c.d. is shown in Fig. 2. It was observed that the intensity of the peaks corresponding to Zn (100) and Zn (103) were the strong for deposit at current density, i = 20 mA cm^{-2}, and was found to decrease as i increased. At i = 50 mA cm^{-2}, the intensity of those peaks have diminished, and a new major peak corresponding to Zn (101) has appeared, which was not a significant one at i = 20 mA cm^{-2}. In Fig. 2, the reflections corresponding to Fe (110) and Fe (211) are attributed to the steel substrate. A minor η phase, and major η phase with crystal orientation Zn (103), may be attributed to the coexistence of two Zn–Ni phases, in accordance with the anodic peaks in the cyclic voltammograms. Thus, X-ray diffraction study demonstrated that the drastic change in corrosion resistance of Zn–Ni CMA coatings is a consequent of different phase structures of the alloy coatings in alternate layers, obtained at different current densities. I.e. the coatings at i = 20, 40 and 50 mA cm^{-2} in respect to the present study [22, 23]. The Zn–Ni CMA coatings were produced with different number of layers while keeping the total thickness same and their corrosion properties were measured.

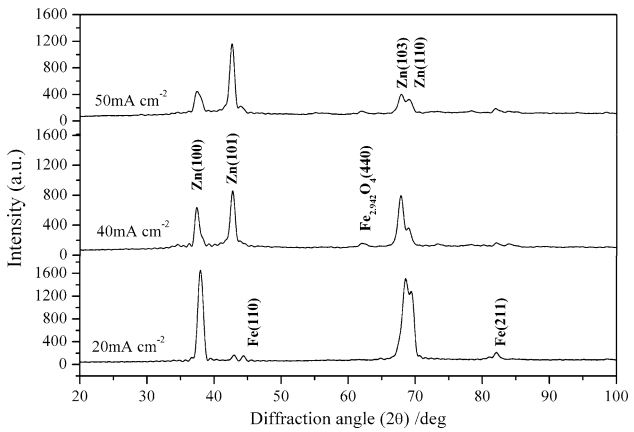

Fig. 2 The XRD patterns of monolithic Zn–Ni alloy obtained at different current densities

3.3 Zn–Ni CMA coating

3.3.1 Optimization of switching cathode current densities

It is well known that, in the case of alloys of zinc with the iron group metals, even a small change in the concentration of the latter may result in significant property change due to change in the phase structure [22]. Bright and uniform monolithic Zn–Ni alloy coatings were developed on mild steel at different c.d., and wt% Ni in the deposit was determined, by stripping the deposit of known mass into dilute HCl solutions followed by colorimetric (spectrophotometric) analysis [24]. In this method, the Ni ions, under proper pH conditions, are made to form a colored complex, by addition of complexing agent, namely, dimethyl glyoxime. The amount of Ni present in solution was evaluated from the standard plot, based on the Beer-Lambertz equation. Consequent to the above facts, wt% Ni in the individual layers were anticipated, while doing multilayer coating. Experimentally, it was found that at i = 20, 30, 40, and 50 mA cm^{-2}, the Zn–Ni bath at optimal composition, produced the coatings having 3.4, 3.8, 5.4 and 10.0 wt% Ni, respectively. The Zn–Ni alloys at different c.d. were developed, and their corrosion stability were evaluated. Among many sets of SCCD's tried (with constant number of layers, typically 4), the corrosion resistances only at 20–40 and 20–50 mA cm^{-2} was found to be less. Hence these sets SCCD's were selected for further layering, and results of which are reported in Table 2.

3.3.2 Optimization of overall number of layers

The properties of CMA electrodeposits, including their corrosion resistance, may often be improved by increasing

Table 2 Effect of layering on corrosion properties of Zn–Ni CMA coatings obtained with 20–40 and 20–50 mA cm^{-2} SCCD's

Configuration	No. of layers	E_{corr} (V)	i_{corr} (μA cm^{-2})	Corrosion rate ($\times 10^{-2}$ mm $year^{-1}$)
$(Zn–Ni)_{30}$	Monolithic	−1.142	14.91	21.4
$(Zn–Ni)_{20/40}$	4	−1.229	5.358	8.39
	6	−1.225	4.404	6.34
	10	−1.155	4.032	5.80
	20	−1.214	1.246	1.79
	60	−1.169	0.383	0.55
	120	−1.049	0.253	0.32
$(Zn–Ni)_{20/50}$	4	−1.116	14.486	20.84
	6	−1.084	12.664	18.23
	10	−1.163	2.525	3.63
	20	−1.146	2.188	3.15
	60	−1.112	0.571	0.82
	120	−0.998	0.276	0.50

the total number of layers, as long as the demarcation between layers is not lost. Therefore, with above two optimal SCCD's, CMA coatings with 6, 10, 20, 60 and 120 layers (the latter, for example, reflects 60 layers from each composition) produced. As evident from Table 2, the corrosion rate decreased as the overall number of layers was increased in both SCCD's. It was found that further increase in number of layers (beyond 120 layers), resulted in decrease of corrosion resistance. The decrease of corrosion rate at higher degree of layering may be attributed to the less relaxation time for redistribution of metal ions (Zn^{+2} and Ni^{+2}) at the diffusion layer, during deposition. I.e. at high degree of layering, the deposition time for each layer is very small. With the result, the metal ions could not relax (against diffusion under given c.d.), and get deposit on cathode with different composition [25]. Hence, at high degree of layering modulation in composition is not likely to take place. In other words, CMA deposit is tending towards monolithic, showing less corrosion resistance. The lowest corrosion rate (0.32×10^{-2} mm $year^{-1}$) was observed for a coating at SCCD of 20–40 mA cm^{-2} with 120 layers. The deposit obtained at 20–50 mA cm^{-2} showed relatively high corrosion rate (0.50×10^{-2} mm $year^{-1}$) as shown in the Table 2. It may be noticed that in spite high wt% Ni content in CMA $(Zn–Ni)_{20/50}$ coating system (10.0 wt% Ni at 50 mA cm^{-2}), the CMA coatings exhibited less corrosion rate, may be due to increased porosity. Therefore, the optimal configuration proposed for best corrosion performance is $(Zn–Ni)_{20/40/120}$.

The improved corrosion resistance of the CMA coatings may be explained in terms of the selective dissolution of alloys in layers, envisaged by Jing et al. [26]. In CMA $(Zn–Ni)_{1/2}$ coating, having different number of layers, the $(Zn–Ni)_2$ top layer (with high wt% Ni) corrode slowly, than the beneath layer $(Zn–Ni)_1$, with low wt% Ni. The failures like pores and crevices occurring in the single layer will be covered by the successively deposited coating layers, and thus the corrosion agents path is longer or blocked [27]. That is why, as the number of layers increased, the corrosive agent needs more time to penetrate through coating defects into the substrate material, than in case of monolithic coating. It can also be interpreted in terms of alternate layers, having different composition, and hence different phase structures [23]. Accordingly, the corrosion protection efficacy of multilayer coatings are due to barrier effect of layers with high wt% Ni, and sacrificial effect of layers with less wt% Ni.

3.3.3 Potentiodynamic polarization study

Figure 3 shows polarization behavior of CMA coatings having $(Zn–Ni)_{20/40}$ configuration having different number of layers. Tafel extrapolation on such curves resulted in determination of the corrosion potential, corrosion current

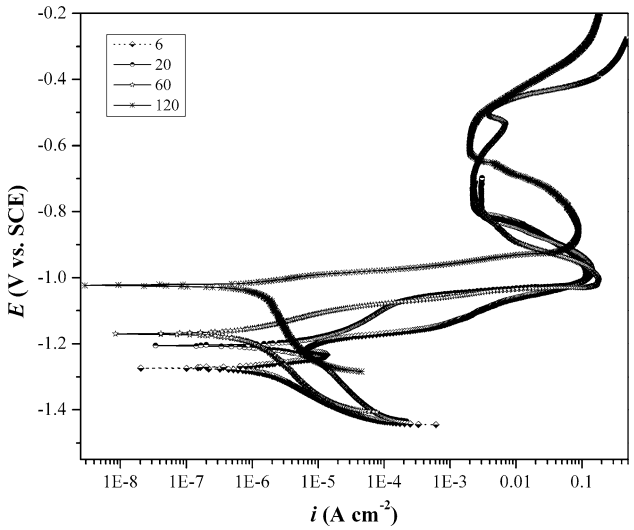

Fig. 3 Potentiodynamic polarization curves of $(Zn–Ni)_1/(Zn–Ni)_2$ CMA coatings with different number of layers (at 1.0 mV s^{-1})

density and corrosion rate, as listed in Table 2. As mentioned before, the increase of the number of layers resulted in a decrease in the corrosion rate. It was found experimentally that wt% Ni in $(Zn–Ni)_{20}$ and $(Zn–Ni)_{40}$ deposits are about 3.4 and 5.4 respectively. Hence, it may be concluded that a small change in wt% Ni in the deposit, is sufficient enough to bring large change in the phase structure of deposits, and hence its corrosion performance.

3.4 Comparison between the corrosion behavior of monolithic and Zn–Ni CMA coatings

The corrosion rates of Zn–Ni alloy coatings with different configurations are given in Table 3. It is apparent that the corrosion rate of the CMA coating with $(Zn–Ni)_{20/40/120}$ configuration is ~60 times lower than that of the monolithic Zn–Ni coating having the same thickness. Further, it was found that CMA coating with $(Zn–Ni)_{20/40/120}$ configuration is more corrosion resistant than CMA $(Zn–Ni)_{20/40/120}$. From the total observed thickness (~15 μm) of $(Zn–Ni)_{20/40/120}$ coating, the average thickness of each layer was found to be in the range 125 nm, shown in Table 3. Thus, it may be concluded that the CMA coating, when designed properly with distinct modulation in composition, better corrosion stability is possible. The comparison of polarization behaviors of monolithic and CMA coatings (both optimal) is shown in Fig. 4. It may be observed that there is considerable decrease in i_{corr} values, when coating is changed form monolayer to multilayer type.

Electrochemical Impedance Spectroscopy, generally known as EIS technique is one of the most powerful tool for studying the electrochemical behavior of the materials. In this technique, Impedance behavior is being studied by the application of an AC signal (sinusoidal wave). The

Table 3 Comparison of corrosion rates of optimized monolithic and CMA Zn–Ni coatings with 120 layers of total same thickness

Coating configuration	Average thickness of the layers (nm)	wt% Ni in alternate layer	E_{corr} (V) vs. SCE	i_{corr} (μA cm^{-2})	Corrosion rate ($\times 10^{-2}$ mm year^{-1})
Monolayer $(Zn–Ni)_{30}$	–	4.2	−1.142	14.91	21.4
CMA $(Zn–Ni)_{20/40/120}$	125	3.4	−1.049	0.253	0.32
		5.4			
CMA $(Zn–Ni)_{20/50/120}$	141	3.4	−0.998	0.276	0.50
		6.5			

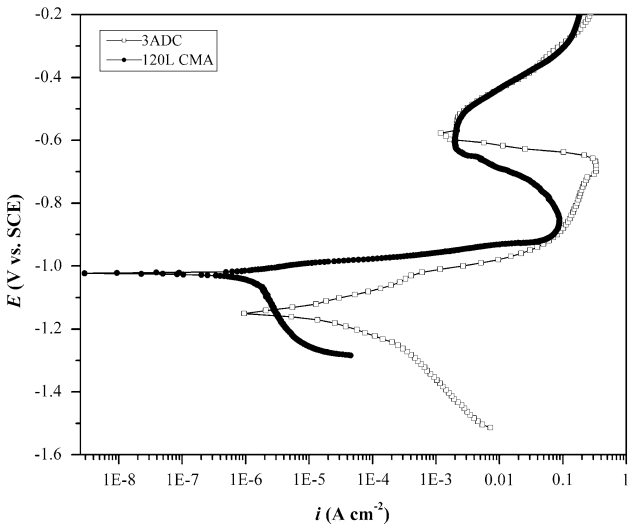

Fig. 4 Comparison of polarization behaviors of monolithic Zn–Ni alloy and CMA $(Zn–Ni)_1/(Zn–Ni)_2$ coatings of same thickness

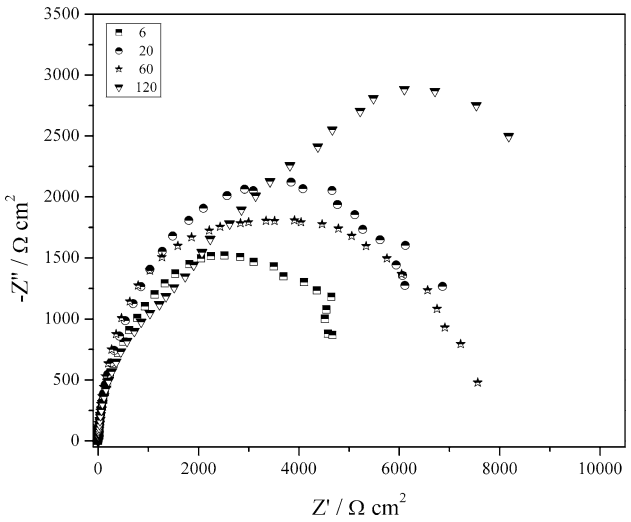

Fig. 5 Nyquist plots of CMA Zn–Ni coating system with $(Zn–Ni)_1/(Zn–Ni)_2$ configuration having different number of layers

form of the current–voltage relationship of the impedance in an electrochemical system can also be expressed as,

$$Z(\omega) = V(t)/I(t) \quad (1)$$

where, $V(t)$ and $I(t)$ are the measurements of voltage and current in an AC system. The impedance spectra of Zn–Ni CMA with different number of layers are as shown in Fig. 5. Comparison of impedance spectra of monolithic $(Zn–Ni)_{30}$ and CMA $(Zn–Ni)_{20/40/120}$ is shown in Fig. 6. The impedance signals shows that the solution resistance, Rs is nearly identical in both cases as the same bath chemistry and cell configuration were used. The considerably high impedance of the CMA coating reflects its higher corrosion resistance. The larger diameter of the (unfinished) semicircle in the case of the CMA $(Zn–Ni)_{20/40/120}$ coating indicates increased corrosion resistance, which is attributed by the change in the film (coating) capacitance. Small capacitive loop of the monolithic alloy at high frequency limit shows its lower corrosion resistance. No diffusion-limited process, in the form of Warburg impedance is observed. A comparative account of corrosion behaviors of monolayer Zn (with corrosion rate, 33.2×10^{-2} mm year^{-1}) and $(Zn–Ni)_{30}$ and CMA $(Zn–Ni)_{20/40/120}$ coatings (all under optimal conditions) is shown in Fig. 7.

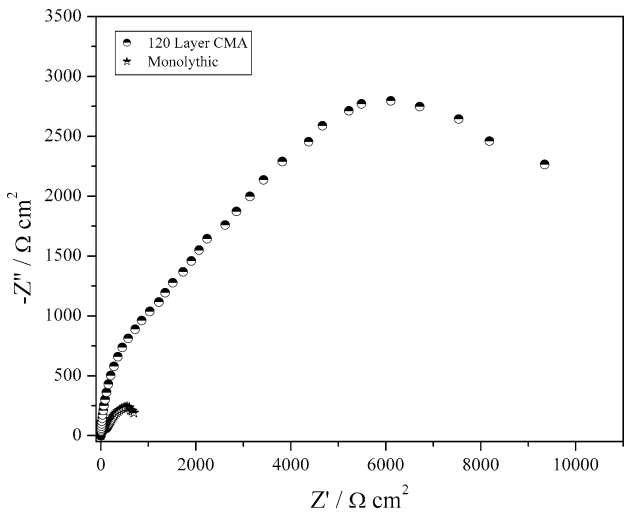

Fig. 6 Comparison of impedance responses of monolithic $(Zn–Ni)_{30}$ and CMA $(Zn–Ni)_{20/40/120}$ coatings under optimal conditions

3.5 AFM and SEM characterization of CMA coatings

Atomic Force Microscopic structures (AFM) of Zn–Ni CMA coatings were analyzed and the mean roughness R_a and root-mean-square roughness Z_{rms} were determined

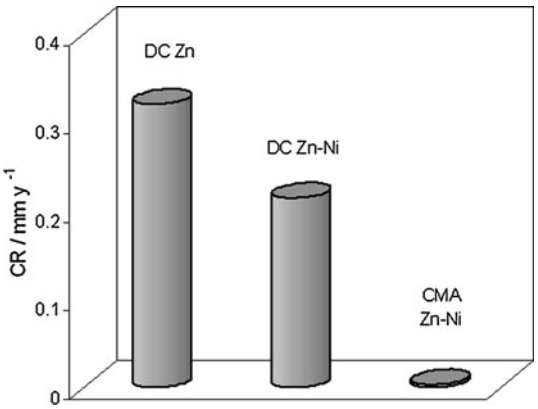

Fig. 7 Comparison of corrosion rates of Zn, Zn–Ni alloy (both monolithic) and Zn–Ni CMA coatings

based on AFM images using the SPIP^{TM} software (Fig. 8). The R_a value was 82 nm and the Z_{rms} values were 107 nm. The Abbott-Firestone curve indicates that the Zn–Ni coating has the less steep peaks and the most uniform roughness distribution. Formation of multiple layers deposited at two different cathode current densities was analyzed by scanning electron microscope (SEM) image. Figure 9a shows the surface structure of the deposit at optimized SCCD's of 20–40 mA cm^{-2}. Cross-sectional view is shown in Fig. 9b. Figure 9c shows the surface morphology of the deposit after corrosion test. It clearly shows that CMA coating has dissolved layer after layer. The alternate layers of Zn–Ni alloys, in which layer with less wt% of noble metal dissolves preferentially than the layer with more wt% of noble metal. In these images the formation of different layers can be observed. It was found that the surface homogeneity of the coatings decrease with increase of layer thickness, due to the availability of excess time for electro crystallization in each layers.

3.6 X-ray Photoelectron Spectral (XPS) characterization of Zn–Ni CMA coating

X-ray Photoelectron Spectroscopy (XPS) measurements were performed in UHV (2.5×10^{-10} Torr base pressure) using 5600 Multi-Technique System (PHI, USA). The samples were irradiated with an Al K_α monochromated source (1486.6 eV) and the outcome electrons were analyzed by a Spherical Capacitor Analyzer using the slit aperture of 0.8 mm. The samples were analyzed at the surface and after sputter cleaning with 4 kV Ar^+ ion gun (sputter rate was $\sim$43 A min^{-1} on the reference SiO_2/Si sample). All the samples were charged at the surface, before sputter cleaning. Neutralizer was used for charge compensation. Additional mathematical shift was used when necessary, to reference all the peaks to C1s at 285 eV.

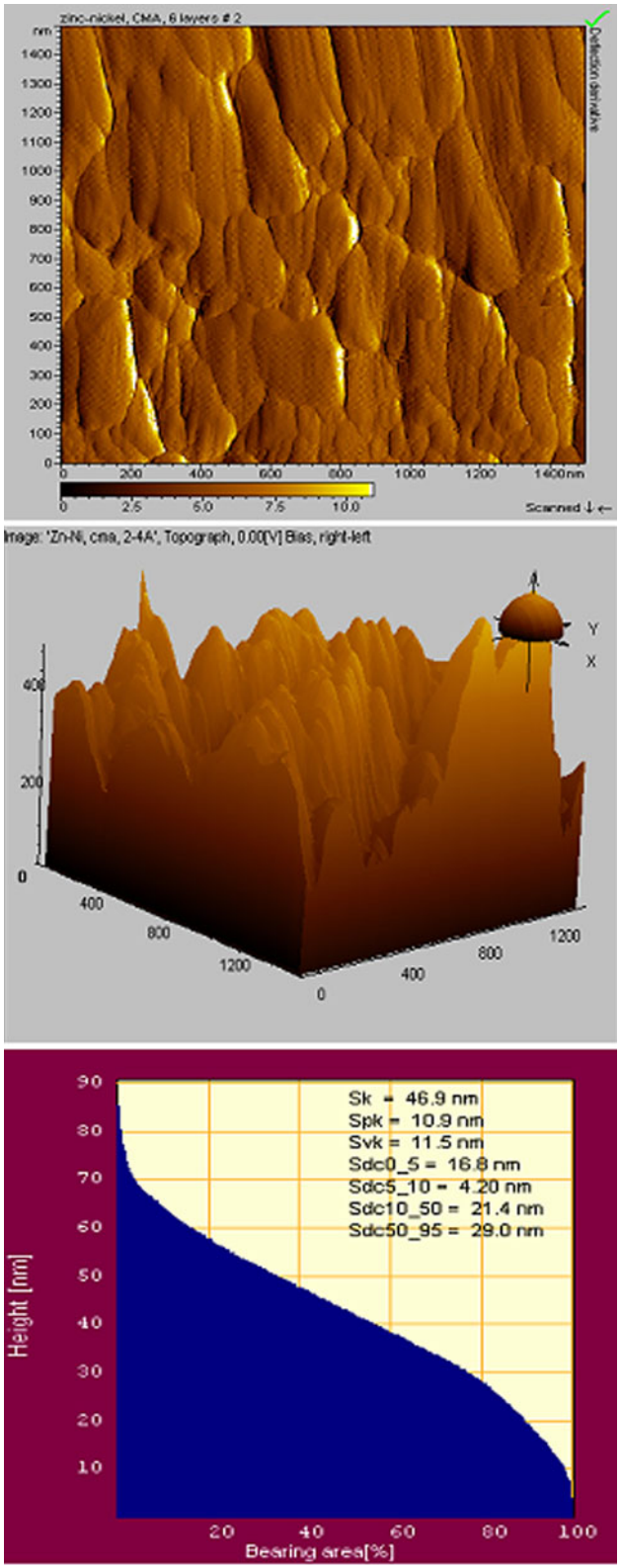

Fig. 8 Atomic force microscopic (AFM) image and surface roughness of monolithic Zn–Ni alloy and CMA $(Zn–Ni)_1/(Zn–Ni)_2$ coatings with six layers

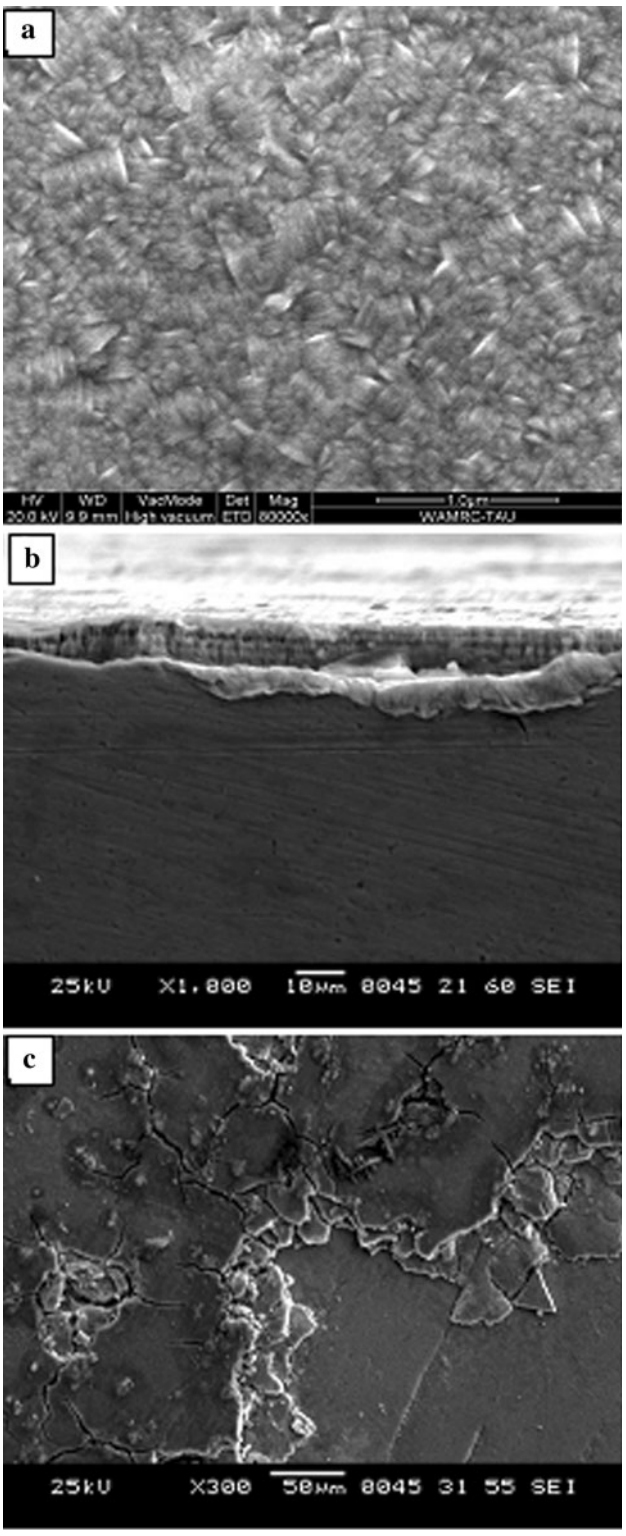

Fig. 9 Cross sectional and Surface SEM images of Zn–Ni CMA coating with six layers

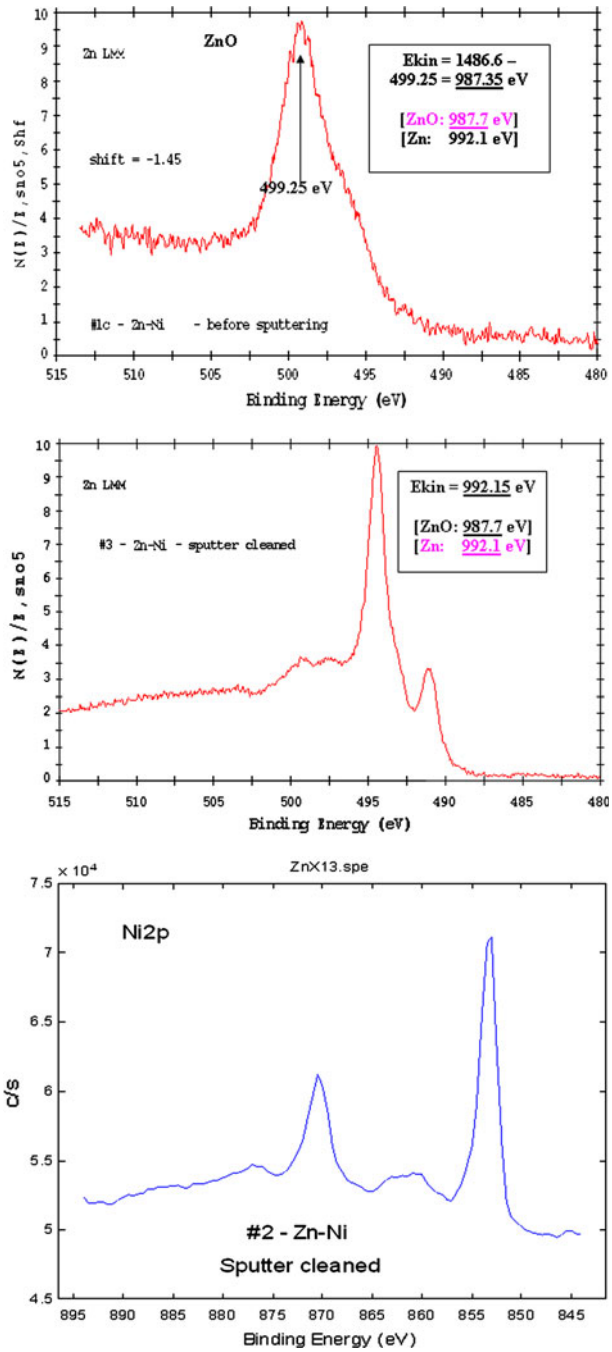

Fig. 10 XPS spectrum of Zn_{LMM} and Ni2p peak of Zn–Ni CMA deposit with six layers at 20–40 mA cm^{-2} SCCD

The discrimination of Zn and ZnO are not possible as the Zn $2p_{3/2}$ spectra are similar for both the non-oxidized and the oxidized metals (1021.6 and 1021.7 eV, respectively). To solve this problem, Auger spectrum of Zn (L3M45M45) was recorded (the kinetic energy for Zn is 992.3 eV, while the energy for ZnO is 987.6 eV). According to the electron energy peaks, nickel found within the outer layer in the non-oxidized form, while zinc was in the oxidized one (Fig. 10). After sputtering in deeper levels, Zn appears as indicated by the energy peak at 992 eV. Nickel, however, was found to be non-oxidized within the concentration profile studied. This result implies

that the corrosion of zinc, as a less noble component, is prevailing during the first corrosion stages, whereas more noble nickel remains non-corroded.

4 Conclusions

The monolayer and cyclic multilayer alloy coatings of Zn–Ni were deposited on mild steel and their corrosion behaviors were studied, and the following conclusions were drawn.

1. Corrosion performance of Zn–Ni alloy coatings can be increased to several folds of its magnitude, by multilayer coating by proper manipulation of coating configuration.
2. CV study demonstrated that gelatin and SA, in combination have improved the homogeneity and brightness of the deposit.
3. The enhanced corrosion stability of CMA Zn–Ni coatings is due to formation of alternate layers of alloys, having different phase structures, consequent to different wt% Ni, evidenced by XRD study.
4. It was found that the CMA Zn–Ni coating at optimal configuration, $(Zn–Ni)_{20/40/120}$ shows $\sim$60 times better corrosion stability, compared to monolayer Zn–Ni alloy of same thickness.
5. Corrosion resistance of CMA coating increases with number of layers only up to a certain optimal level (120 layers), and then decreased. It is due to the fact that, at higher degree of layering the CMA coating becomes monolithic, due to interlayer diffusion.
6. XPS study showed that that the corrosion of zinc, as a less noble component, is prevailing during the first corrosion stages, whereas more noble nickel remains non-corroded.
7. The corrosion protection efficacy of multilayer coatings are due to barrier effect of layers with high wt% Ni, and sacrificial effect of layers with less wt% Ni.

Acknowledgments The authors thank Prof. Noam Eliaz, School of Mechanical Engineering, Tel-Aviv University, Israel for support in carrying out few analyses. We also thank Mario Levinstein from the Biomaterials and Corrosion Lab for his machinery and AFM work and Zahava Barkay, Larisa Burstein and Yuri Rosenberg from the Wolfson Applied Materials Research Center for their help.

References

1. Gabe DR, Green WA (1998) Surf Coat Technol 105:195
2. Nabiyouni G, Schwarzacher W, Rolik Z, Bakonyi I (2002) J Magn Magn Mater 253:77
3. Eliaz N, Gileadi E (2008) In: Vayenas CG, White RE, Gamboa-Aldeco ME (eds) Modern aspects of electrochemistry, vol 42. Springer, New York, pp 191–301
4. Brenner A (1963) Electrodeposition of alloys. Principles and practice, vol II. Academic Press, New York, p 589
5. Venkatakrishna K, Thangaraj V, Chitharanjan Hegde A (2008) Indian J Chem Technol 15:252–258
6. Orinakova R, Turonova A, Kladekova D, Galova M, Smith RM (2006) J Appl Electrochem 36:957–972
7. Chawa G, Wilcox GD, Gabe DR (1998) Trans Inst Met Finish 76:117
8. Krishan KSR, Srinivasan K, Mohan S (2002) Trans Inst Met Finish 80(2):46
9. Haseeb A, Celis J, Roos J (1994) J Electrochem Soc 141:230
10. Despic AR, Jovic VD (1989) J Electrochem Soc 136:1651
11. Kalantary MR (1994) Plat Surf Fin 81:80
12. Thangaraj V, Eliaz N, Chitharanjan Hegde A (2009) J Appl Electrochem 39:339–345
13. Barral G, Maximovitch S (1990) Colloque de Physique 51(14): PC4–PC291
14. Kalantary MR, Wilcox GD, Gabe DR (1998) Br Corr J 33:197
15. Liao Y, Gabe DR, Wilcox GD (1998) Plat Surf Fin 85(3):60
16. Liao Y, Gabe DR, Wilcox GD (1998) Plat Surf Fin 85(8):62
17. Liao Y, Gabe DR, Wilcox GD (1998) Plat Surf Fin 85(9):88
18. Kirilova I, Ivanov I, Rashkov St (1998) J Appl Electrochem 28:637
19. Kirilova I, Ivanov I, Rashkov St (1998) J Appl Electrochem 28:1359
20. Kirilova I, Ivanov I (1999) J Appl Electrochem 29:1133
21. Thangaraj V, Ravishankar K, Chitharanjan Hegade A (2008) Chin J Chem 26:1
22. Stimming U (1986) Electrochim Acta 31:415
23. Ganeshan P, Kumaraguru SP, Popov BN (2007) Surf Coat Technol 201:7896
24. Vogel AI (1951) Quantitative inorganic analysis. Longmans Green and Co, London
25. Nasser K (2006) Electroplating: Basic principles, processes and practice. Elsevier Ltd, Berlin
26. Fei J-Y, Wilcox GD (2006) Surf Coat Technol 200:3533
27. Dobrzanski LA, Lukaszkowicz K, Pakula D, Mikula J (2007) Arch Mater Sci Eng 28:12